Evaluation of critical factors affecting the thermal performance of metal curtain walls by simulations

H. Ge, M.A.Sc and P. Fazio, Ph.D., P.Eng., FCSCE, FASCE
Centre for Building Studies
Department of Building, Civil and Environmental Engineering
Concordia University
huagezh@cbs-engr.concordia.ca fazio@vax2.concordia.ca

ABSTRACT

An integrated method is employed in this paper to study the relative influence of certain design details on the thermal performance of metal curtain walls. Results from the programs FRAME/VISION, used to simulate the heat transfer across the wall systems, show that varying the configurations in the frame, can significantly improve the thermal performance of curtain walls. For example, the U-factor of the frame can be reduced as much as 60% by using a larger thermal break. The impact of the stainless steel screws is significant as well, and can reduce the U-factor of the frame by up to 16% when the standard spacing of 152mm is applied.

A simplified correlation model developed by Cornick & Sander is used to evaluate the effect of different improvement strategies for curtain wall systems on the energy consumption of a prototype office building subject to Montreal weather conditions. The results suggest that for curtain wall systems with poor frame performance, the simple use of high performance glazing unit would not yield significant improvement. Only when the frame performance is improved, the benefits of high performance glazing units are fully realized.

INTRODUCTION

Metal-glass curtain walls are commonly used in high-rise buildings due to the advantages of high-quality control in fabrication and construction, lightweight, space saving, and significant aesthetic freedom. However, their thermal performance is still low and in practice they are normally referred to as "heat sink" due to their high thermal transmittance. The trend towards reducing energy consumption and improving indoor thermal comfort, has induced the industry to use high performance glazing units to improve the thermal performance of metal curtain walls. However, the benefits provided by high performance glazing units can be greatly reduced by the poor performance of the frame and the spandrel panels. Figure 1a shows the joint section of a standard metal curtain wall system. Three main thermal bridges exist at this section including the conventional aluminum spacer at the edge of the glazing, the steel screws used to fasten the pressure plates to the frame, and the return of the steel back-pan. The heat flux plotted in Figure 1b shows the main paths for heat loss through the joint section. These thermal bridges significantly lower the thermal performance of metal curtain walls. Griffith (1998) studied the thermal bridge effect produced by the screws and concluded that the thermal bridge effect depends on material and spacing of the screws. The simulations performed by Carpenter (1994) indicated that the U-factor for the edge-of-spandrel, which is the perimeter area within 63.5mm of the frame, is 7.5 times of that at the center-of-spandrel. A study conducted by Enermodal Engineering Ltd. (1994) found that "despite having half its area in spandrel panel, the curtain wall total U-factor is slightly higher than a standard double-glazed window".

Metal curtain walls initially grew within metal window industry and the current methodology and standards developed for evaluating window performance are also used for curtain walls. For decades, metal curtain walls have been treated as windows plus walls. The U-factor of metal curtain walls has been represented only by the U-factor of the vision panel. For the wall section, only the center of the insulated spandrel panel is considered with the effect of edge-of-spandrel and frame ignored. The new edition of Canadian Standard A440.2 (CSA 1998) recommends evaluating both the vision panel and the spandrel panel, but separately.

Metal curtain walls differ from windows in that they have a much larger continuous glazing portion, more complex configuration at the joints, and more complex connection between frame and the spandrel panels. As indicated in the cross-section shown in Figure 1a, to separate the glazing section from the spandrel section may be an oversimplification and the U-factor evaluated in accordance with CSA A440.2 procedure or the U-factor calculated conventionally

may cause discrepancy when estimating energy consumption for metal curtain wall buildings.

Although studies have recognized the effects of some of the thermal bridges, no comprehensive study has emerged in our survey that treats a metal curtain wall as an integrated system and addresses all the factors affecting its thermal performance. This paper presents an integrated method to calculate the overall U-factor of metal curtain walls. The objectives of this study include:

1. Evaluating the critical factors affecting the thermal performance of metal curtain walls by simulations using programs FRAME/VISION;
2. Evaluating the impact of thermal characteristics of metal curtain walls on the energy consumption using a simplified energy simulation model.

METHODOLOGY

The conventional way to calculate the thermal transmittance of metal curtain walls includes an area weighted U-factor for the vision panel, and a U-factor for the center-of-spandrel. The new edition of CSA A440.2 (1998) recommends taking the spandrel panel into account, but "The properties for curtain walls shall be determined separately for the vision panel and the spandrel panel." As shown in Figure 2, the dimension to determine the U-factors is to the outside of the mullions. The section to be simulated is the jamb section (Figure 2a, & 2b), which has an adiabatic boundary condition for the frame-wall junction.

The significant thermal bridge effect of the return of the steel back-pan makes the assumption of adiabatic boundary condition for the frame-wall joint unrealistic. A holistic approach, which treats curtain walls as integrated systems, is employed in this paper and it is referred to as the integrated method. As shown in Figure 3 the dimensions to determine the overall U-factor for the wall are the horizontal and vertical distances between the centerlines of the mullions. The sections to be simulated for this calculation include the sill section (Figure 3a), the intersection of the vision panels (Figure 3b), and the intersection of the spandrel panels (Figure 3c). Thus, the boundary conditions are the real conditions experienced by the curtain wall sections.

FACTORS AFFECTING THE OVERALL U-FACTOR

To study the thermal bridge effect at the joint section (Figure 1a), the programs FRAME and VISION (EE1995) are employed to carry out the simulations. FRAME is a 2-dimensional finite volume program to evaluate the heat transfer through window frames. It can also be used to simulate the wall junction. VISION is a one-dimensional program to simulate the heat transfer through center-of-glass. The integrated approach described in the section above is used. Only the sill section is simulated.

Two different types of curtain wall systems with different design details are studied. The main difference between these two types of curtain walls is the mullion configurations. The first one is a standard system, which uses a thin strip of nylon as thermal break at the mullion nose, referred to as system A in this paper (Figure 4a). The second is an improved system referred to as system B and it has a much larger thermal break achieved by replacing the aluminum mullion nose with reinforced nylon (Figure 4b). The parameters studied include different types of glazing units, different types of spacers, different designs of the steel back-pan, and the screw spacing.

Two types of glazing units are considered. The first one is a standard double insulated glazing unit (IGU), which is composed of double 6.4mm thick clear glass with 12.7mm air gap with a conventional aluminum spacer. The U-factor of the center-of-glass obtained from the VISION simulation is 2.76 W/(m^2·K). The second one is a high-performance IGU, which has low-E coating (ε=0.1) on the exterior surface of the inner pane, Argon gas filling within the glazing cavity, and a thermally broken spacer. The U-factor of the center-of-glass obtained from the VISION simulation is 1.53 W/(m^2·K). The spandrel panels are composed of 6.4mm thick exterior clear glass and 101.6mm high-density mineral fiber insulation with a 19mm air gap in between. The U-value of the center-of-spandrel is 0.34 W/(m^2·K). Two designs of back-pan connection are considered. One is the regular design (Figure 4), the other is the revised design, which shifts the connection to the interior flange of the mullion tube to eliminate the thermal bridge created by the return of the back-pan. The detailed configurations are listed in Table 1 and illustrated in Figure 4.

The boundary conditions used for the simulations are CSA winter conditions: warm side T_i= 21°C, h_i=8.3 W/(m^2·K); cold side T_o= -18°C, h_o= 30 W/(m^2·K). The screws are made of stainless steel with conductivity of 14.3 W/m·K and the standard spacing is 152 mm from center-to-center. For system A, both

parallel path and isothermal plane methods are used to simulate the effect of screws. The parallel path method requires two simulation runs; one with steel screw, the other without. These two runs result in two sets of U-values for edge-of-glass, frame, and edge-of-spandrel. The U-factor for each component is obtained by area weighting the value from each run. The stainless screw has a diameter of 6.4mm with 12.7mm head. Considering the fin effect created by the screw, 12.7mm is used as the characteristic dimension to calculate the area weight of the section with screws. The isothermal plane method requires the determination of the effective conductivity for the screw space, which is an area-weighted average of the screw conductivity and the no-screw conductivity. Since the parallel path and isothermal plane results provide the lower and upper bounds and the real results fall between these two, the average of these two results is used for the comparisons. For system B, the use of the reinforced nylon mullion nose eliminates the thermal effect of screws. The pre-simulation shows that the effect of the screws in system B is less than 0.5%, so only the configuration with screws is simulated.

The U-factors obtained through the simulations for various design details for system A are listed in Table 2. The improvements are calculated over the base configuration with a standard IGU and a regular back-pan design. The simulation shows that the U-factor for the edge-of-glass depends mainly on the spacer type and the U-factor for the center-of-glass. The configuration of the back-pan has little impact due to the high heat loss through the frame. The type of glazing unit has little influence on the U-factor of the frame (2.5%) and on the U-factor of the edge-of-spandrel (2.4%). Although the use of high-performance IGU can lower the U-value at the edge-of-glass by 32%, the effect on the total U-value of the joint section is only 9.6%. The revision of the back-pan lowers the U-factor for the frame by about 14%, but it dramatically increases the U-factor for the edge-of-spandrel by about 50%. The net result on the total U-value of the joint section is 0%, which indicates that the shifting of the backpan would not reduce the heat loss unless the conductance of the frame is improved, which is the case in system B.

The effect of the spacing of stainless screws for system A with standard IGU, and regular back-pan is indicated in Table 3. The comparisons are made against the case without screws given in the last column of Table 3. The spacing varies from 76mm up to 457mm. As in the back-pan design, the spacing of the screws has little effect on the U-value at the edge-of-glass (1.2%). However, the effect of the screw spacing is significant on the U-factor for the frame and for the edge-of-spandrel (Figure 5). In practice, the pressure plates are normally pre-drilled every 76mm (3”). The standard spacing for screws is 152mm (6”). When the spacing is reduced to 76mm, the U-factor of frame is increased by as much as 27% compared to the case without screws. Sometimes at the corners, to increase the structural strength, screws are used every 76mm, thus decreasing thermal performance. When compared to the standard design (152mm), the increase of screw spacing can reduce the U-factor for the total joint section. When the spacing of screws is increased to 457mm, which is 3 times the standard spacing, the U-factor for the joint section can be reduced by 6.7%. It can be seen that the stainless steel screws at 152mm spacing increase the U-factor of the frame by 16 %. The thermal performance of the frame may be improved by increasing the screw spacing, by using low-conductivity screw materials, and by breaking the thermal bridge.

The U-factors for various design details of system B are listed in Table 4. The improvements are calculated over the base configuration of standard IGU and regular back-pan design. Same as for system A, the U-factor of the edge-of-glass depends mainly on the spacer type and the U-factor for the center-of-glass. With the improvement of the frame performance, the dependency of the U-factor at the edge-of-glass on the frame configuration is slightly greater than that in system A. The performance of the frame is also more sensitive to the type of glazing. The use of high-performance IGU lowers the total U-factor for the joint by about 20%, which is much greater than that for system A. The revised back-pan lowers the U-factor for the frame by 16% and the total U-factor for the joint section by 6%. These results indicate that when the frame performance is improved, the shifting of the backpan connection can reduce the heat loss through the joint section.

The use of the reinforced nylon mullion nose reduces the U-factor of the frame by 58~62%, the U-factor of edge-of-spandrel by 56~61%, and the total U-factor of the joint section by 44~52% compared to system A (Table 5). With the higher thermal resistance in the frame, the impact of spacer type on the U-factor of the edge-of-glass, frame, and edge-spandrel increases.

ENERGY CONSUMPTION FOR A PROTOTYPE OFFICE BUILDING IN MONTREAL

A simplified energy model developed by Cornik and Sander (1995) is employed to study the impact of thermal characteristics of metal curtain walls on heating and cooling loads for a prototype office building in Montreal. This model is composed of a set of regression equations derived from a database of 5400 DOE-2.1E simulations for 25 Canadian locations. It served as the basis for prescriptive and trade off procedure in the Modeling National Building Energy Code (MNBEC, 1997). The predicted annual energy use from this model is within 10% of the detailed DOE-2.1E simulations.

Only the four exterior zones facing the cardinal orientations excluding the core are considered in this model. The building envelope is characterized by three parameters: thermal transmittance (U), Solar gain parameter (V), and internal gain parameter (W), which are defined as:

$$U = (U_g \cdot A_g + U_w \cdot A_w)/A_t \quad \text{W/m}^2\cdot\text{K} \quad (1)$$

$$V = A_g \cdot SC_g/A_t \quad \text{dimensionless} \quad (2)$$

$$W = I \cdot A_f/A_t \quad \text{W/m}^2 \quad (3)$$

where

A_w = opaque wall area, m^2;
A_g = window wall area including frame, m^2;
A_t = gross wall area, $A_w + A_g$, m^2;
A_f = floor area associated with envelope, typically 4.5m deep, m^2;
U_w = opaque wall U-factor, $W/m^2\cdot K$;
U_g = window U-factor, including frame, $W/m^2\cdot K$;
SC_g = window shading coefficient, dimensionless;
I = design heat gain from lights, people, and equipment, W/m^2 floor area.

The heating load predicted by this model includes an annual heat loss, which is a linear function of U with the slope and intercept dependent on the climate, and modifiers to consider the heating reduction due to solar and internal gains. Similarly, the predicted cooling load also includes two parts, a base cooling, which is a linear function of V and W, and a modifier to account for the effect of U.

The prototype building simulated is a 20-storeys high office building with dimension of 30m by 30 m. The floor-to-floor height is 3.66m. The glazing wall ratio is 50%. Only the perimeter zones facing four cardinal orientations are considered and the depth of the perimeter zone is 4.5m. The inputs for this model include the thermal characteristics of building envelope, U, V, internal gain W, and a series of climate-dependent correlation coefficients. The climate-dependent correlation coefficients for 25 Canadian cities are listed in Cornik and Sander (1994).

The dimension of the curtain wall is 1.22m wide and 1.83m high at centerline of mullions for both vision panel and spandrel panel. Four different types of curtain wall designs are chosen for the energy consumption simulation. The determined parameters U, V, W are listed in Table 6 for each design. The U-factor is determined using the integrated scheme illustrated in Figure 3. The shading coefficient for the vision panel includes the effect of frame. The solar heat gain coefficient (SHGC) for the glass is obtained from the VISION program, and the SHGC for the frame is calculated in accordance with the CSA A440.2 standard. The internal gain parameter W is determined in accordance with ASHRAE 90.1 (1992). The simulation results are shown in Figure 6.

From Table 6 it can be shown that the use of high-performance glazing units can reduce the overall U-factor by 25% for system A although the high performance glazing unit provides 45% lower U-value (1.53 $W/m^2\cdot K$) at the center-of-glass than the standard glazing unit (2.76 $W/m^2\cdot K$). The total energy consumption can be reduced by 15% (Figure 6). By replacing frame system A with frame system B, the U-factor can be reduced by 22% and energy consumption by 22% as well, which is even higher than using high performance glazing units. This indicates the importance of improving frame performance. When the high performance frame system are combined with the high performance glazing unit, the overall U-factor can be reduced by 48%, and the energy consumption can be reduced by 30%.

CONCLUSIONS

An integrated method used in this paper shows the relative influence of the design details on the thermal performance of metal curtain walls. The simulation results indicate that the frame configuration (e.g. the depth and materials of the thermal breaks in the frame section) has a significant impact on the U-factor. For example, the use of the reinforced nylon mullion nose can reduce the U-factor of the frame by as much as 60%. For a curtain wall assembly sized 1.22m wide by 3.66m high, by using the frame system with a larger thermal break, the overall thermal transmittance can be reduced by 22%, and the corresponding energy saving for a prototype

office building in Montreal is about 22%, which is even higher than replacing the standard IGUs with high-performance glazing units. The effect of shifting backpan connection depends on the performance of the frame. For the standard curtain wall system, no improvement can be made on the total U-value of the joint section from the revision of backpan, but when the frame performance is improved, the total U-value at the joint section can be reduced by 6%. For the standard curtain wall system, the impact of the stainless steel screws is significant as well, and can increase the U-factor of the frame by 16% when the standard spacing of 152mm is applied.

A simplified model has been used to evaluate the energy consumption of a prototype office building with different curtain wall designs. The simulation results indicate that the performance of the frame is very important. For the standard curtain wall system A, 8.5% frame area contributes 30% to the overall U-factor. With the poor performance of the frame and edge-of-spandrel, simply using high-performance glazing units would not make significant improvement on the overall thermal resistance and on the energy consumption. The energy consumption of the curtain wall is dramatically reduced when the frame performance is improved together with the use of high-performance glazing units.

ACKNOWLEDGEMENTS

The writers express their appreciation to the Natural Sciences and Engineering Research Council (NSERC) of Canada and the Fonds pour la Formation des Chercheurs et l'aide à la Recherche (Fonds FCAR) of Québec for their financial support and to Kawneer Company Canada Ltd. for providing the design and materials for related test specimens.

REFERENCES

Carpenter, S. and A.H. Elmahdy, 1994. Thermal performance of complex fenestration systems. *ASHRAE Transations*, Vol. 100(2), pp.1179-1186.

Cornick S., D. M. Sander, 1994. "Development of heating and cooling equations to predict changes in energy use due to changes in building envelope thermal characteristics". IRC Report 656, NRCC, Ottawa.

Cornick, S.M. and Sander, D.M., 1995. "A simplified energy model for analysis of building envelope thermal characteristics." Proceedings of Thermal Performance of the Exterior Envelopes of Buildings VI, pp.687-695.

CSA. 1998. Energy Performance of Windows and Other Fenestration Systems, *CAN/CSA A440.2. Canadian Standard Association.*

Enermodal Engineering Ltd., 1994. "Thermal Performance of Complex Fenestration Systems: Skylights, Greenhouse Windows and Curtainwalls", CANMET Report.

Enermodal Engineering Ltd., 1995. FRAMEplus toolkit, version 4.0. Enermodal. Kitchener, Ontario.

Griffith, B.T., Finlayson, E.U., Yazdanian M. and Arasteh D. 1998. The Significance of Bolts in the Thermal Performance of Curtain-Wall Frames for Glazed Facades, *ASHRAE Transactions* 104 (1): 1063-1069.

MNBEC, 1997. Modeling National Building Energy Code.

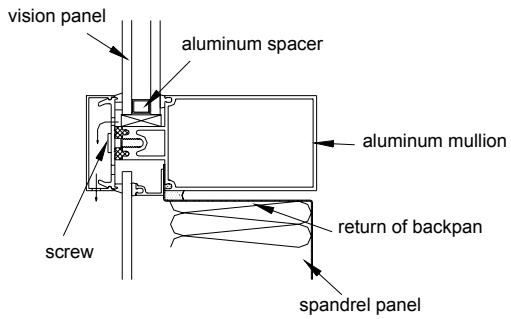

Figure 1a Joint section of a standard metal curtain wall

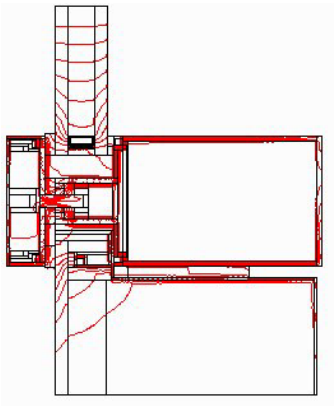

Figure 1b Heat flux across the joint section

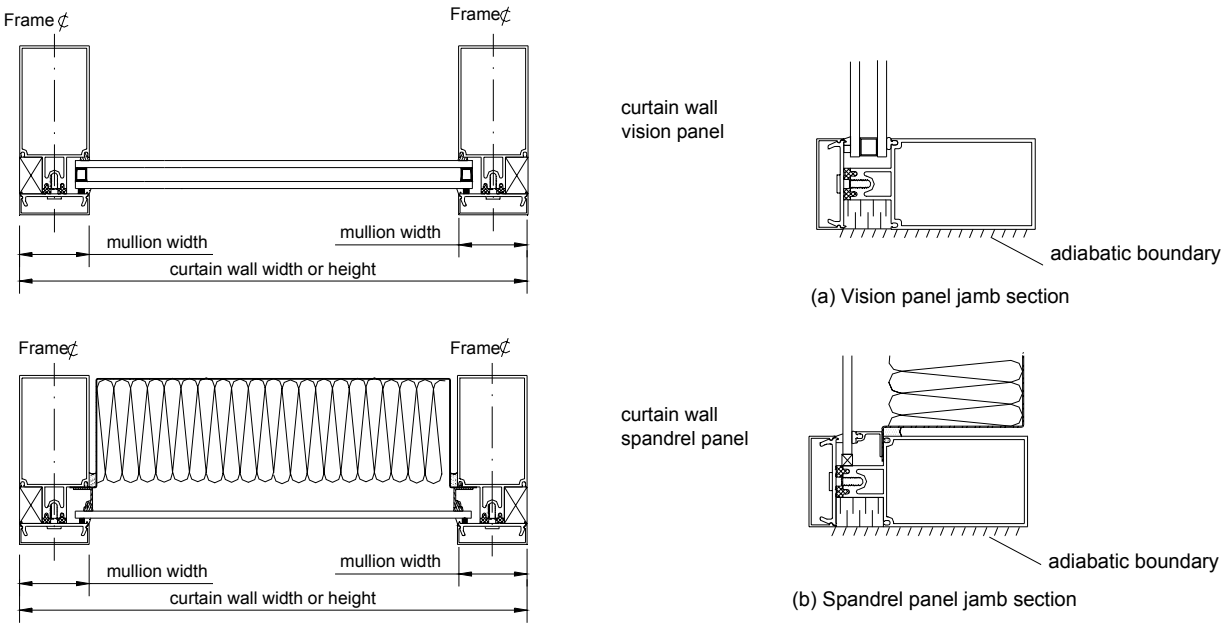

Figure 2. The CSA method to determine the U-factor for curtain wall

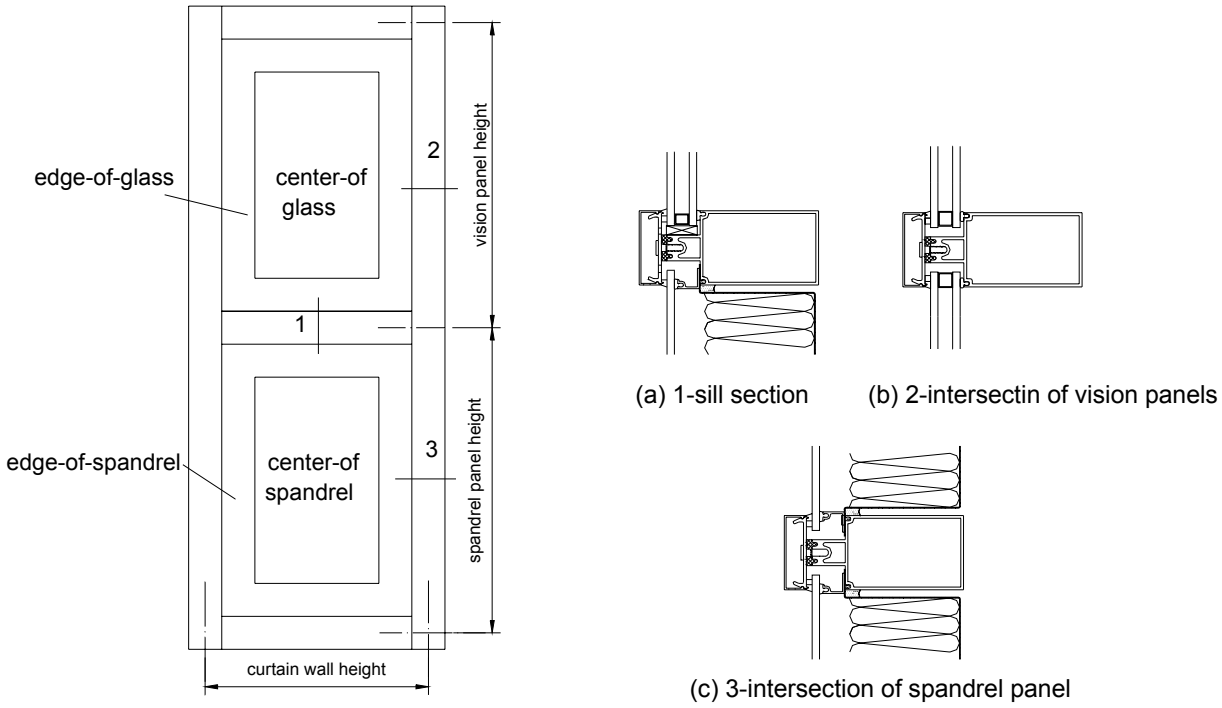

Figure 3. The integrated method to calculate the overall U-factor for a curtain wall section

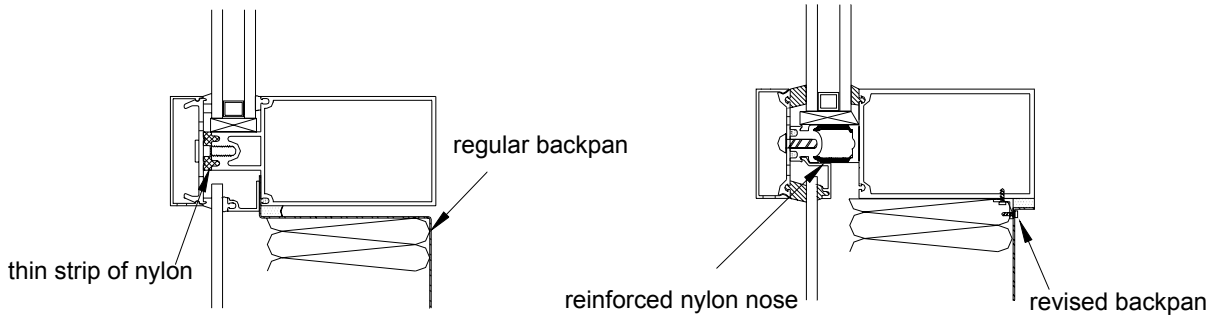

Figure 4. Curtain wall configurations simulated

Table 1 Detailed configurations simulated

	Configurations			A	B
1	clear double glazing unit with conventional aluminum spacer	Regular backpan design	screw spacing at 150mm	√	√
2			screw spacing at 76mm, 230mm, 300mm and 450mm	√	
3		Revised backpan design with screw spacing of 150mm		√	√
4	double glazing unit with low-E coating, Argon gas, and thermally broken spacer	Regular backpan design with screw spacing at 150mm		√	√
5		Revised backpan design with screw spacing at 150mm		√	√

Table 2. U-factors in W/(m^2 · K) for various design details for system A *

	Regular Back-pan			Revised Back-pan			
	Standard IGU	**High-performance IGU**	**IM (%)**	**Standard IGU**	**IM (%)**	**High-performance IGU**	**IM (%)**
U_{e-g}	3.18	2.17	31.8	3.27	-2.8	2.20	30.8
U_{frame}	8.24	8.03	2.5	7.13	13.5	7.00	15.1
U_{e-s}	2.07	2.02	2.4	3.10	-49.7	3.07	-48.3
U_{total}	4.50	4.07	9.6	4.50	0.0	4.09	9.1

* IM= improvement, IGU=insulated glazing unit, U_{e-g} = U-factor of the edge-of-glass, U_{e-s} = U-factor of the edge-of-spandrel. The comparisons are over the base case "Standard IGU, Regular back-pan".

Table 3. Effect of screw spacing on the U-factors in W/(m^2·K) for system A with standard IGU *

		Spacing of screws (mm)					
		76	**152**	**229**	**305**	**457**	**No screw**
Edge-of-glass	**U-factor (W/m^2·K)**	3.22	3.18	3.18	3.18	3.18	3.18
	Difference (%)	1.2	0.0	0.0	0.0	0.0	
Frame	**U-factor (W/m^2·K)**	9.03	8.24	7.90	7.72	7.51	7.10
	Difference (%)	27.2	16.0	11.3	8.8	5.8	
Edge-of-spandrel	**U-factor (W/m^2·K)**	2.23	2.07	1.99	1.96	1.89	1.82
	Difference (%)	22.7	13.6	9.5	7.5	3.9	
Total	**U-factor (W/m^2·K)**	4.83	4.50	4.36	4.29	4.20	4.03
	Difference (%)	19.8	11.6	8.2	6.4	4.1	
U_{total} Compared to the standard spacing 152mm (%)		-7.4	0.0	3.0	4.6	6.7	10.3

*compared to the base case "No screw".

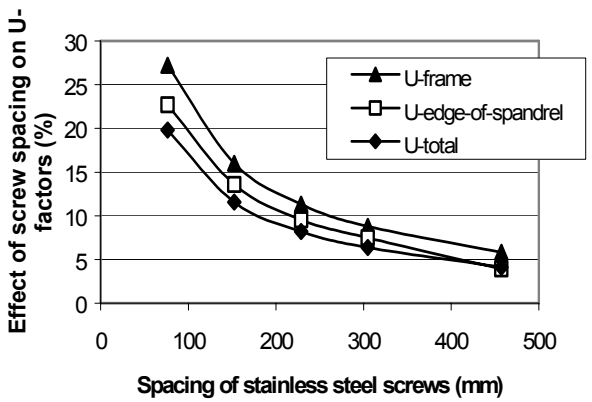

Figure 5. Impact of screw spacing on U-factor at the joint section for system A with standard IGU, regular back-pan

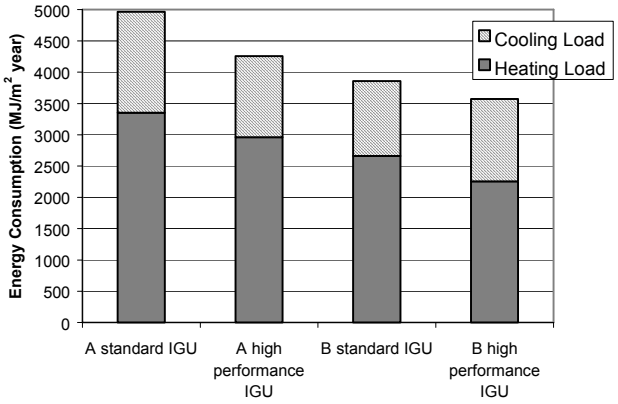

Figure 6 Comparison of energy consumption among four different curtain wall designs

Table 4. U-factors in W/(m^2 · K) for various design details for system B *

	Regular back-pan			Revised Back-pan			
	Standard IGU	High-performance IGU	IM (%)	Standard IGU	IM (%)	High-performance IGU	IM (%)
U_{e-g}	3.24	2.10	35.2	3.07	5.3	1.93	40.4
U_{frame}	3.46	3.18	8.1	2.9	16.2	2.67	22.8
U_{e-s}	0.91	0.85	6.6	1.19	-30.8	1.19	-30.8
U_{total}	2.54	2.04	19.7	2.39	5.9	1.93	24.0

* IM= improvement, IGU=insulated glazing unit, U_{e-g} = U-factor of the edge-of-glass, U_{e-s} = U-factor of the edge-of-spandrel. The comparisons are over the base case "Standard IGU, Regular back-pan".

Table 5. Comparisons of U-factors in W/(m^2 · K) between system A and system B*

	Regular Back-pan								Revised back-pan			
	Standard IGU				High-performance IGU				High-performance IGU			
	U_{e-g}	U_f	U_{e-s}	U_{total}	U_{e-g}	U_f	U_{e-s}	U_{total}	U_{e-g}	U_f	U_{e-s}	U_{total}
A	3.18	8.24	2.07	4.50	2.17	8.03	2.02	4.07	2.20	7.00	3.07	4.09
B	3.24	3.46	0.91	2.54	2.10	3.18	0.85	2.06	1.93	2.67	1.19	1.93
IM (%)	-1.9	58.0	56.0	43.6	3.2	60.4	57.9	49.4	12.3	61.9	61.2	52.8

*U_{e-g} = U-value of edge-of-glass, U_{e-s} = U-value of edge-of-spandrel

Table 6. Input parameters for energy consumption simulations

Configurations			U W/(m^2 · K)	V dimensionless	W W/m^2
A	**1**	Standard IGU	2.31	0.45	30.20
	2	High performance IGU	1.74	0.31	
B	**3**	Standard IGU	1.80	0.44	
	4	High performance IGU	1.21	0.29	